MODE I FATIGUE AND FRACTURE OF ADHESIVELY-BONDED PULTRUDED GFRP DOUBLE CANTILEVER BEAMS

Moslem Shahverdi, Anastasios P. Vassilopoulos, Thomas Keller

Composite Construction Laboratory (CCLab), Ecole Polytechnique Fédérale de Lausanne (EPFL), Station 16, Bâtiment BP, CH-1015 Lausanne, Switzerland
**e-mail address: anastasios.vasilopoulos@epfl.ch*

Keywords: Pultruded GFRP laminates, Fatigue, Energy release rate, Adhesively-bonded joints.

Abstract

A series of fatigue experiments was performed in order to investigate the effect of the R-ratio on the fatigue/fracture behavior of adhesively-bonded pultruded GFRP double cantilever beam joints. Constant amplitude fatigue experiments were carried out under displacement control with a frequency of 5 Hz in ambient laboratory conditions. Five different R-ratios were applied: R=0.1, R=0.3, R=0.5, R=0.65 and R=0.8. The dominant failure mode was a fiber-tear failure that occurred in the mat layers of the pultruded laminates. The depth of the crack location significantly affected the energy dissipated for the fracture under cyclic loading. Fatigue crack growth curves were derived for each R-ratio and each observed crack path location. An empirical fatigue crack growth formulation for the modeling of constant amplitude Mode I fatigue behavior of the examined adhesively-bonded pultruded double cantilever beam joints under different R-ratios is introduced and validated. The model can potentially be used for the derivation of fatigue crack growth curves under any different R-ratio assisting the development of methodologies for the fatigue life prediction of the examined joints under realistic loading conditions.

1 Introduction

The most common way of representing the fatigue data of composite materials and structural components, and design based on phenomenological modeling concepts, is the S-N curve. When the design is based on micromechanics modeling and a crack or cracks develop inside the material, the matrix crack density or delamination are normally conceived as being an acceptable damage metric.

The literature comprises a vast number of publications e.g. [1] on the aforementioned topics. For composite laminates the S-N curves are usually derived under given loading conditions in order to model the constant amplitude fatigue behavior of the examined materials. A significant effect of the stress ratio, $R=\sigma_{min}/\sigma_{max}$, on fatigue life has been reported in literature and extensively investigated to establish theoretical models for the subsequent prediction of fatigue life under more complicated loading conditions such as block and variable amplitude loading [2].

Extensive research efforts were also devoted to the investigation of the fatigue crack growth under Mode I [3], Mode II [4], and mixed-Mode [5] fracture of composite joints under fatigue loading. Instead of the S-N curves, fatigue crack growth (FCG) curves are used to represent

the fatigue behavior and also provide information concerning the developed damage in terms of crack or cracks that propagate during fatigue loading. The FCG curves are plots of the strain energy release rate, G, versus the crack propagation rate, da/dN, usually on logarithmic axes. The strain energy release rate, SERR or G, is usually the most appropriate fracture parameter for composite materials, and hence has been used by many researchers.
Fatigue crack growth curves show three different regions. The first, corresponding to lower SERR values, designated subcritical, is located close to the fatigue threshold where cracks propagate very slowly. The middle part, which is linear, covers most of the FCG curve and a constant crack growth rate gradient is observed in this region. Finally, a rapid crack growth rate region is observed where the cyclic SERR approaches the critical SERR of the examined material with fast crack propagation.
Although the shape of the derived FCG curves was similar for several different material and structural systems, contradictory results were found in the literature concerning the effect of the R-ratio on the derived curves. Moreover, in a lot of published works, only the middle part of the FCG curves is examined, since it is difficult to derive experimentally the fast part of the FCG curve, difficult to capture rapid crack propagation, and time- consuming to estimate the fatigue threshold.
Paris et al. [6] observed that in the second region, the relationship between the crack propagation rate, da/dN, and the stress intensity factor range, ΔK, or the maximum stress intensity factor, K_{max}, follows a power law equation. Martin and Murri [3] introduced a phenomenological equation that is able to model the FCG behavior over the entire range of applied G, from the first to the third region. The derived model, designated the "total fatigue life model", expresses the crack growth rate as a function of the maximum cyclic strain energy release rate, G_{max}, the strain energy release rate threshold, G_{th}, and the critical strain energy release rate, G_c.
In the present work, the fracture behavior of adhesively-bonded pultruded GFRP DCB joints is experimentally investigated under constant amplitude fatigue loading patterns with different displacement ratios. The effect of the applied R-ratio on the resulting fatigue crack growth curves is thoroughly analyzed and correlated to the exhibited failure processes of the specimens. The effect of the different locations of the crack path on the fracture behavior of the examined joints is also investigated as was done in a previous publication [7] by the authors for quasi-static loading.
An empirical fatigue crack growth formulation for the modeling of constant amplitude Mode I fatigue behavior of adhesively-bonded pultruded glass fiber-reinforced polymer DCB joints under different R-ratios is introduced in this study. The model was established based on existing experimental data and was validated by comparisons to new fatigue/fracture experimental results. It is shown here that if the model parameters are estimated accurately, the model can be used for the derivation of reliable FCG curves for several unknown loading conditions and can therefore assist the development of methodologies for the fatigue life prediction of joints under realistic loading conditions.

2 Experimental program

2.1 Material

Adhesively-bonded pultruded GFRP DCB joints were examined under constant amplitude fatigue loads. The laminates, supplied by Fiberline A/S, Denmark, consisted of E-glass fibers embedded in isophthalic polyester resin and had a width of 40 mm and thickness of 6.0 mm. The laminates comprised two outer combined mat layers and a roving layer in the symmetry plane. The fiber architecture of the laminates is shown in Fig. 1. The longitudinal strength and

Young's modulus of the GFRP laminate were obtained from tensile experiments, according to ASTM D3039-08, as being 307.5±4.7 MPa and 25.0 ±0.5 GPa respectively.
A two-component epoxy adhesive system was used, Sikadur 330, supplied by Sika AG Switzerland, as the bonding material. The tensile strength of the adhesive was 39.0 MPa and the stiffness 4.6 GPa.

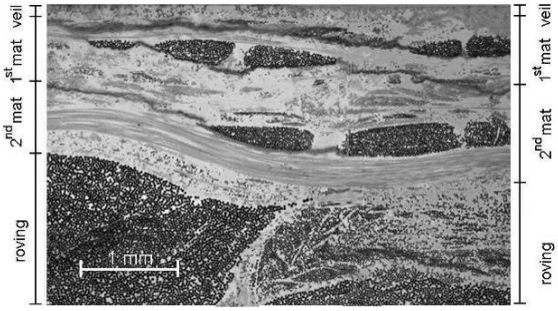

Figure 1. Fiber architecture of upper half of laminate cross section, transverse to pultrusion direction

2.2 Specimen geometry and fabrication
The geometry of the DCB specimens used is shown in Fig. 2. The specimen length was 250 mm including a pre-crack length of 50 mm. All surfaces subjected to bonding were mechanically abraded by approximately 0.3 mm to increase roughness and then chemically degreased using acetone. An additional 0.5 mm was abraded from the upper arm only along the pre-crack in order to ensure that the crack would propagate between the two mat layers of the upper pultruded laminate [8]. An aluminum frame was employed to assist the alignment of the two pultruded laminates. The 2-mm thickness of the adhesive was controlled by using spacers embedded in the bonding area. In-house developed piano hinges were glued, using the same epoxy adhesive, at the end of both specimen arms to allow load application. A Teflon film of 0.05-mm thickness was placed between the upper arm and the adhesive layer to introduce the pre-crack. After preparation of the configuration, the specimens were kept under laboratory conditions for 24 hours and then placed for 24 hours in a conditioning chamber at 35°C and 50±10% RH to ensure full curing of the adhesive.

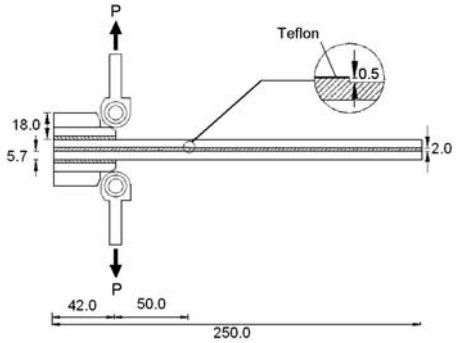

Figure 2. Specimen configuration, dimensions in mm

2.3 Experimental set-up and loading
A 25-kN MTS Landmark servo-hydraulic testing rig, calibrated to 20% of its maximum capacity, was used for all the fatigue experiments. All experiments were conducted in laboratory conditions, 23±5°C and 50±10% RH, under displacement control at a frequency of 5 Hz. Three different *R*-ratios were selected to cover a wide range of possible loading conditions: *R*=0.1 representing fatigue loading with high amplitude values, an intermediate

case, R=0.5, and R=0.8 to represent fatigue loading with low amplitude and high mean cyclic stresses. Those experimental data were used for the development of the model, while the modeling results were validated by comparisons to experimentally derived FCG curves under two different R-ratios: R=0.3 and R=0.65.

The experimental process followed three steps:

Step 1: The specimen was inserted into the grips of the machine and aligned. The load that was introduced due to the clamping process, less than 5 N, was manually set to zero by adjusting the position of the moving rod of the testing rig.

Step 2: After specimen installation a loading ramp was applied to initiate and propagate the crack up to around 15-30 mm.

Step 3: The fatigue loading was started at a maximum displacement equal to the maximum displacement reached during the quasi-static loading in order to record the initial fast crack propagation values corresponding to the fast crack growth rate region.

A schematic representation of the loading procedure, steps 2 and 3, is shown in Fig. 3.

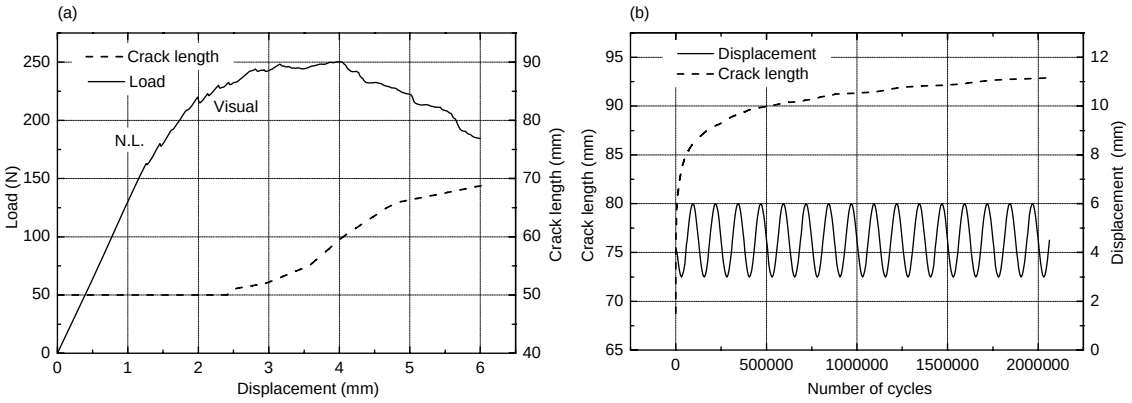

Figure 3. Schematic illustration of loading process, (a) quasi-static loading, step 2, and (b) cyclic loading, step 3

3. Experimental results

3.1 Failure modes

In all the examined specimens the observed failure mode, according to ASTM D 5573-99, was a fiber-tear failure or light-fiber-tear failure. The crack paths were located between the two lower mat layers of the upper laminate as planned, therefore corresponding to Path II, according to the nomenclature given in [8]. However, two different failure modes were observed: one when the crack was propagating in the upper CSM of the first mat layer, Path II-A, and another when the crack was propagating in the lower CSM of the second mat layer, Path II-B.

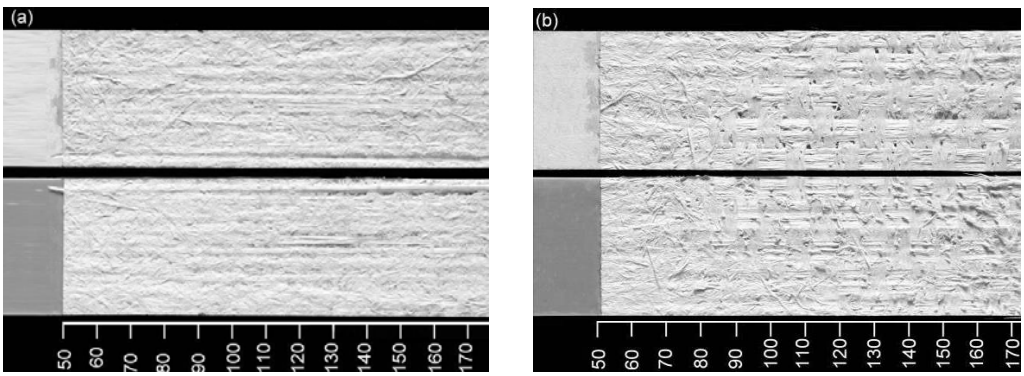

Figure 4. Crack surface comparisons: (a) Path II-A, DCB0.1-02a, (b) Path II-B, DCB0.1-01

Examples of typical failure surfaces with crack growth along Path II-A, and Path II-B are shown in Fig. 4. Regarding the morphology of the fracture surfaces of the specimens under Mode I fatigue loading, a clear difference between the generated fracture surfaces is observed when the crack propagation location changes [8]. The Path II-B surface shows much more fiber tear than Path II-A.

3.2 Compliance and crack length measurements

The relationship between specimen compliance and crack length is required in order to estimate the SERR. The compliance of the specimen, C, defined as the ratio of the maximum displacement over the maximum load (δ_{max}/P_{max}), can be calculated at each number of cycles directly from the recorded data. However, derivation of the crack length during fatigue loading is not an easy task. Direct methods, crack gages and visual observation, and also indirect methods, e.g. the dynamic compliance calibration, exist for this purpose. As proved in [8] the dynamic compliance calibration method could be applied to all specimens and for cracks running along the total length of the joints. Therefore it was used for derivation of the compliance vs. crack growth rate relationship and calculation of the SERR values in the present work.

4 Fracture mechanics data analysis

4.1 Crack growth rate calculation

The 7-point incremental polynomial fitting, according to ASTM E647-08, was used to calculate the crack growth rate. The incremental polynomial method fits a second-order polynomial to sets of a specified number of successive data points, usually 3, 5, 7 or 9. The slope of the determined equation at any point corresponds to the crack propagation rate.

4.2 Strain energy release rate calculation

The strain energy release rate of the DCB joints can be calculated based on linear elastic fracture mechanics. According to this theory, for a DCB joint with width B and an existing crack length, a, the SERR is a function of the maximum cyclic load, P_{max}, and the rate of the compliance change, dC/da:

$$G_{I\max} = \frac{P_{\max}^2}{2B}\frac{\mathrm{d}C}{\mathrm{d}a} \tag{1}$$

Standard methods for the SERR calculation are based on this equation, the difference between them basically being the way in which the derivative dC/da is obtained. A thorough analysis of the applicability of several methods for the calculation of the SERR to similar composite joints is presented in [9]. It was shown in [9] that for similar pultruded GFRP DCB joints, all methods give similar results with the exception of simple beam theory. Therefore, in the present work, the experimental compliance method is used according to which the measured compliance is fitted to the measured crack length by a power law equation of the form: $C=ka^n$. The maximum cyclic SERR can then be calculated as:

$$G_{I\max} = \frac{nP_{\max}\delta_{\max}}{2Ba} \tag{2}$$

Correction factors for the loading blocks and moments resulting from large displacements were applied according to ASTM 5528-01 (2007).

4.3 Fatigue crack growth curves

The FCG curves for all the examined *R*-ratios are shown in Fig. 5 for Path II-A and Path II-B. The results prove that the relationship between G_{Imax} and d*a*/d*N* is highly dependent on the *R*-ratio. Regardless of the crack path location, a steeper curve reaching a higher fatigue threshold corresponds to higher *R*-ratios.

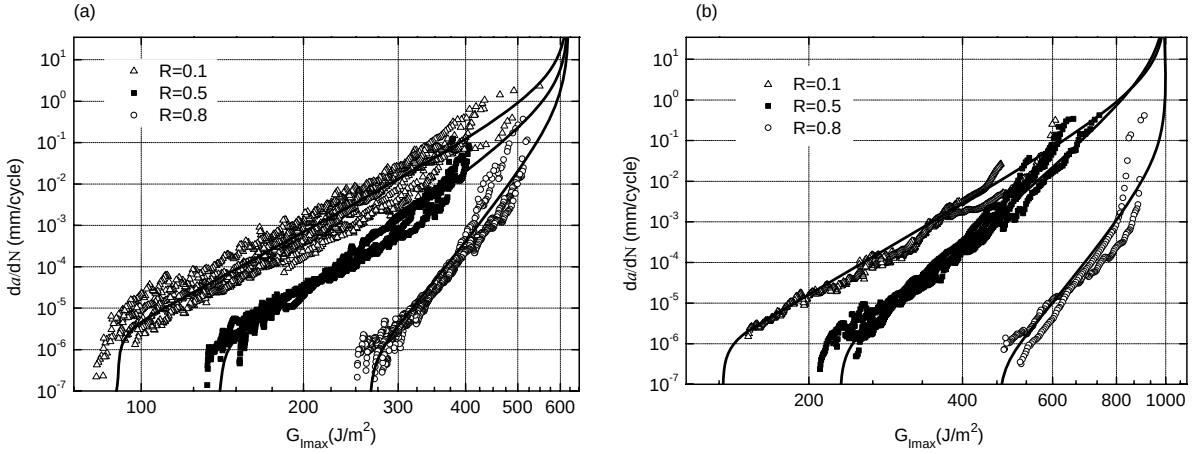

Figure 5. Crack growth rate versus G_{Imax} for (a) Path II-A, (b) Path II-B, solid lines are plots of model results

Initially fiber bridging occurs for all specimens independent of the *R*-ratio, therefore, for all experiments where the crack propagates along the same path a similar SERR value is calculated. As the experiment developed however, for lower *R*-ratios the crack closure was breaking the fibers that bridged the crack faces and consequently the energy required for subsequent crack propagation was reduced. Therefore, the differences between FCG curves under different *R*-ratios were more pronounced close to the fatigue threshold. The effect of the crack path location is also visible in these graphs, The corresponding FCG curves were shifted to higher SERR values when the path changed from Path II-A to Path II-B.

5. Modeling

The introduced model, Eq. (3), resembles the total fatigue life model [3] with parameters *D*, *m*, and G_{Ith} being functions of the *R*-ratio. For the examined DCB joints, the *D*, *m*, and G_{Ith}, model parameters were estimated by fitting Eq. (3) to the available experimental data for three different *R*-ratios, i.e. *R*=0.1, 0.5 and 0.8, for both Path II-A and Path II-B (see solid lines in Fig. 5):

$$\frac{da}{dN}(R) = D(R)\left(G_{\mathrm{Imax}}\right)^{m(R)} \frac{\left(1-\left(\frac{G_{\mathrm{Ith}}(R)}{G_{\mathrm{Imax}}}\right)^{25}\right)}{\left(1-\left(\frac{G_{\mathrm{Imax}}}{G_{\mathrm{Ic}}}\right)^{3}\right)} \tag{3}$$

The following functional forms were derived from the experimental data:

$$D(R) = A_1 e^{B_1 R^2} \tag{4}$$

$$m(R) = A_2 R^2 + B_2 \tag{5}$$

$$G_{\mathrm{Ith}}(R) = A_3 R^2 + B_3 \tag{6}$$

Parameters A_i and B_i in Eqs. (4-6) are derived by linear regression analysis after plotting the derived values of D, m, and G_{Ith} against the square of the R-ratio. The FCG curve for each desired R-ratio can be derived by Eq. (3) after substitution of the functions from Eqs. (4-6).
The predicted FCG curves for R-ratios equal to 0.3 and 0.65, corresponding to Path II-A crack propagation based on the model, are plotted in Fig. 6 by solid lines.

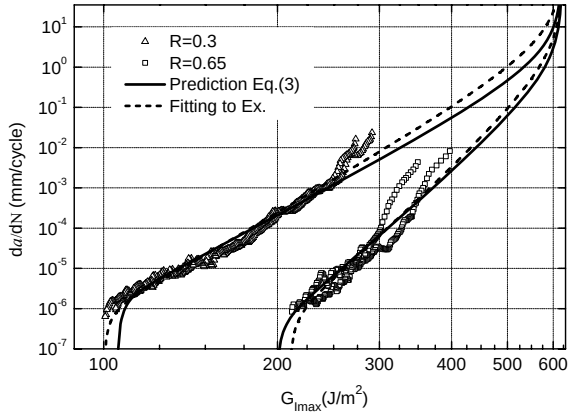

Figure 6. Modeling validation by comparison of experimental results and modeling prediction for Path II-A at R=0.3 and R=0.65

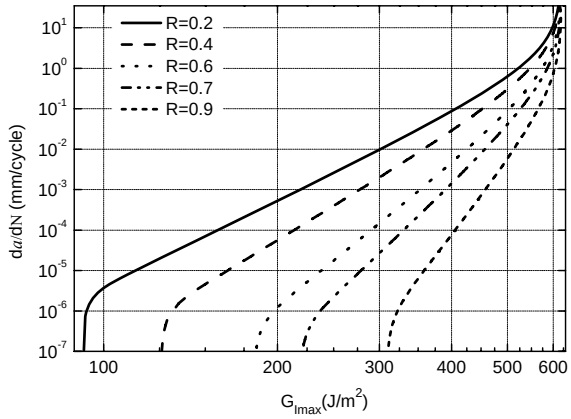

Figure 7. Predicted FCG curves at various R-ratios for Path II-A based on proposed model

The new total life fatigue model can be used for the derivation of other FCG curves, under different R-ratios, and for different crack paths, e.g. Path II-A and Path II-B, as long as the base line fatigue data exist and allow derivation of the relationships between the model parameters and R-ratio used.
Predicted FCG curves for different R-ratios corresponding to Path II-A crack propagation are shown in Fig. 7. Such curves can be used for crack length estimation under block and variable loading conditions.

6. Conclusions

The fatigue fracture behavior of double cantilever beam specimens was experimentally examined under the displacement ratios R=0.1, 0.3, 0.5, 0.65 and 0.8 in order to investigate the effect of the different R-ratios on the derived fatigue crack growth curves.

Fatigue crack growth curves exhibited high dependence on the R-ratio independent of the SERR fatigue parameter used for the representation. The FCG curves corresponding to higher R-ratios exhibited higher slopes in the middle part resulting in higher fatigue threshold values. When plotted on the G_{Imax}-da/dN-plane they all reach the same maximum value, similar to that of the critical strain energy release rate derived from quasi-static experiments.

A total fatigue life model that takes into account the effect of the R-ratio on the FCG curve has been introduced. The derivation of the new model is phenomenological, relying on the fitting of the existing total life fatigue model to experimental data under different R-ratios in order to estimate the necessary model parameters as functions of the R-ratio. The new model was used for the modeling/prediction of the fatigue and fracture behavior of the examined joints under five different R-ratios. The results proved that the model could accurately simulate the behavior of the examined material and was also capable of predicting the behavior exhibited under unseen loading conditions, i.e. different than the R-ratios used for estimating the model parameters.

References

[1] Philippidis T.P., Vassilopoulos A.P. Complex stress state effect on fatigue life of GRP laminates. Part I, experimental. *Int J Fatigue*, **24**(8), pp. 813-823 (2002).

[2] Vassilopoulos A.P., Manshadi B.D., Keller T. Influence of the constant life diagram formulation on the fatigue life prediction of composite materials. *Int J. Fatigue*, **32**(4), pp. 659-669 (2010).

[3] Martin R.H., Murri G.B. *Characterization of mode I and mode II delamination growth and thresholds in AS4/PEEK composites*, in: "*Composite materials: testing and design, ASTM STP 1059*" edited by Garbo S.P. American Society for Testing and Materials, Philadelphia, pp. 251-270 (1990).

[4] Tanaka K., Tanaka H. *Stress-ratio effect on mode II propagation of interlaminar fatigue cracks in graphite/epoxy composites*, in: "*Composite Materials: Fatigue and Fracture ASTM STP 1285*" edited by Armanios E.A. American Society for Testing and Materials, Philadelphia, pp. 126-142 (1997).

[5] Naghipoura P., Bartscha M., Voggenreitera H. Simulation and experimental validation of mixed mode delamination in multidirectional CF/PEEK laminates under fatigue loading. *Int J Solids Struct*, **48**(6), pp. 1070-1081 (2011).

[6] Paris P.C., Gomez M.P., Anderson W.E. A rational analytic theory of fatigue, *Trend Eng*, **13**(1), pp.9-14 (1961).

[7] Shahverdi M., Vassilopoulos A.P., Keller T. A phenomenological analysis of Mode I fracture of adhesively-bonded pultruded GFRP joints, *Eng Fract Mech*, **78**(10), pp. 2161-2173 (2011).

[8] Shahverdi M., Vassilopoulos A.P., Keller T. Experimental investigation of R-ratio effects on fatigue crack growth of adhesively-bonded pultruded GFRP DCB joints under CA loading, *Comp part-A*, doi.org/10.1016/j.compositesa.2011.10.018, in press (2011).

[9] Zhang Y., Vassilopoulos A.P., Keller T. Mode I and II fracture behavior of adhesively-bonded pultruded composite joints, *Engng Fract Mech*, **77**(1), pp. 128–143 (2010).